Lab on a Chip

Miniaturisation for chemistry, physics, biology, materials science and bioengineering

www.rsc.org/loc

Volume 12 | Number 19 | 7 October 2012 | Pages 3523–3830

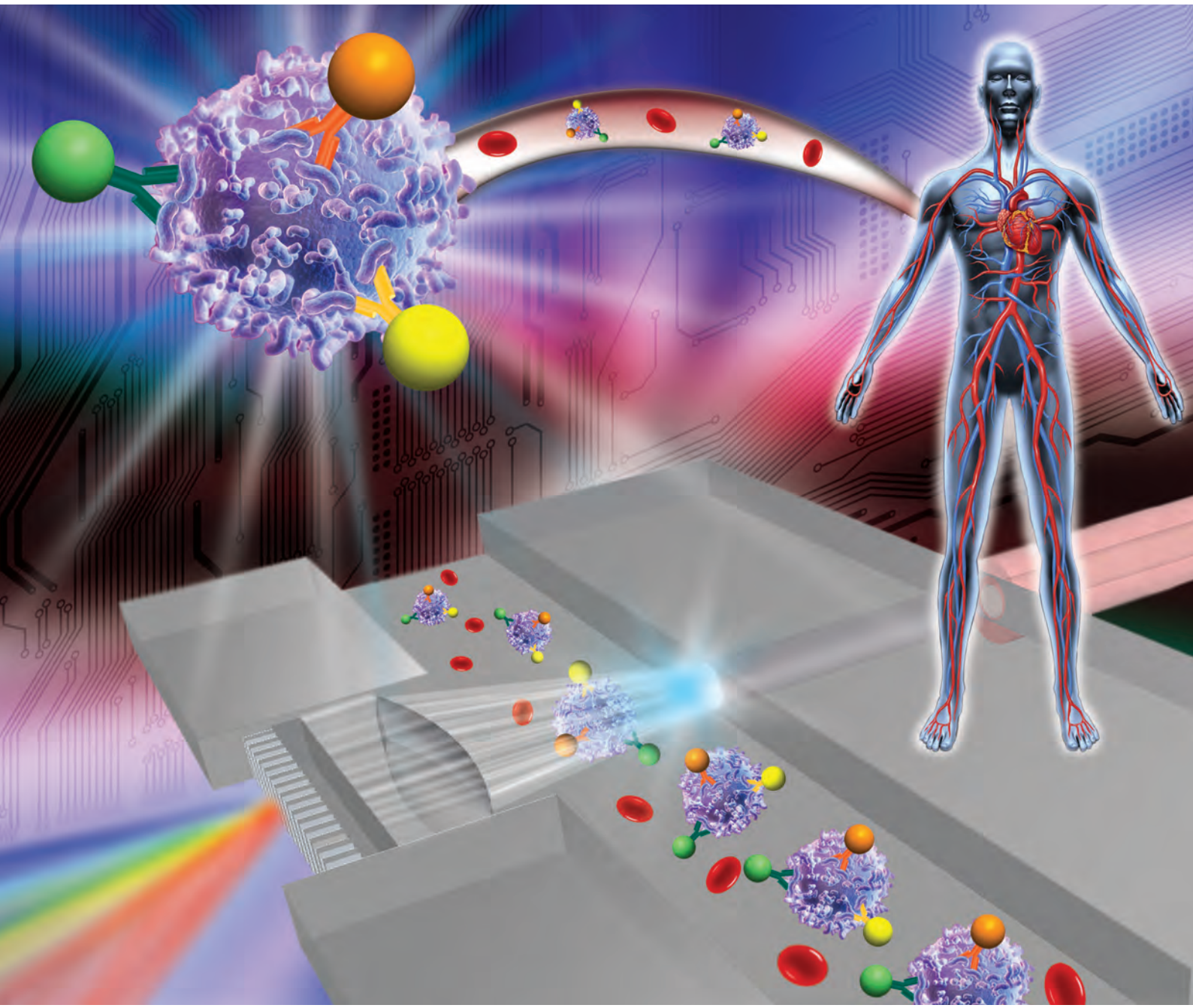

ISSN 1473-0197

RSC Publishing

CRITICAL REVIEW

Wenjun Zhang, Katsuo Kurabayashi *et al.*

Optofluidic detection for cellular phenotyping

1473-0197(2012)12:19;1-U

Lab on a Chip

Dynamic Article Links

Cite this: *Lab Chip*, 2012, **12**, 3552–3565

www.rsc.org/loc

CRITICAL REVIEW

Optofluidic detection for cellular phenotyping†

Yi-Chung Tung,[a] Nien-Tsu Huang,[b] Bo-Ram Oh,[b] Bishnubrata Patra,[c] Chi-Chun Pan,[a] Teng Qiu,[d] Paul K. Chu,[e] Wenjun Zhang*[f] and Katsuo Kurabayashi*[bg]

Received 4th May 2012, Accepted 12th June 2012
DOI: 10.1039/c2lc40509a

Quantitative analysis of the output of processes and molecular interactions within a single cell is highly critical to the advancement of accurate disease screening and personalized medicine. Optical detection is one of the most broadly adapted measurement methods in biological and clinical assays and serves cellular phenotyping. Recently, microfluidics has obtained increasing attention due to several advantages, such as small sample and reagent volumes, very high throughput, and accurate flow control in the spatial and temporal domains. Optofluidics, which is the attempt to integrate optics with microfluidics, shows great promise to enable on-chip phenotypic measurements with high precision, sensitivity, specificity, and simplicity. This paper reviews the most recent developments of optofluidic technologies for cellular phenotyping optical detection.

1. Introduction

A large number of processes, functions, and traits at the cell level serve as important indicators of diseases. For example, a cell under a diseased condition experiences alterations and shows heterogeneity in its gene expression,[1,2] drug resistance,[3,4] protein/metabolite production,[5–7] proliferation,[8] and optical properties.[9,10] The terminology of ''cellular phenotyping'' refers to a scientific process to quantify these disease indicators and other phenotypes affected by the genetic information and environment of a cell. In cellular phenotyping, *individual* cells are isolated from tissue and treated as models for complex human biology. This approach offers a practical alternative to the use of human patients in studying the genetic and long-term environmental influences on the human body (Fig. 1). Current studies reveal that knowledge of the gene alone does not provide any direct insight into downstream biological effects.[11,12] The question of how the genetic factor, coupled with variability in environmental effects (for example, smoking, diet, and atmospheric quality), will affect our bodies and determine the fate of our health still remains unanswered. Establishing links between genetic variants and environmental factors on biological processes is crucial to overcome these challenges and establish personalized medicine.[2] Cellular phenotyping is the key to reveal such links as well.

Optical technologies are powerful tools to measure spatial and temporal variations of cellular phenotypes in a non-destructive manner with high sensitivity and high throughput. Optofluidics, a rapidly emerging research field, has successfully demonstrated the synergistic integration of optical systems with microfluidics.[13–16] Full monolithic integration of miniature optical and fluidic components together on a common microfluidic platform ultimately offers significant advantages, including (a) enhanced sensing performance coupled with increased precision control and fluidic manipulation of cells, (b) portability and usability (and disposability in some cases) that permit point-of-care operations under limited resources without large and expensive instruments and specifically trained operators, and (c) instrumentation cost savings that lead to reduced barriers against wider use. Rapid, low-cost optofluidic detection of abnormalities in particular cellular phenotypes may open ways for effectively screening and preventing cancer, human immunodeficiency virus (HIV) infection, and other deadly diseases. As the notable shift in emphasis occurs from solely genotype-focused studies to genotype-phenotype relationship investigations in current life sciences research, it is important to examine the relevance of optofluidics to cellular phenotyping.

This paper critically reviews recent developments of optofluidic technologies in the past few years, specifically targeting cellular phenotyping applications. We cover four optical techniques: (1) fluorescence detection, (2) surface enhanced Raman spectroscopy (SERS), (3) surface plasmon resonance (SPR), and (4) interferometry as representative methods employed in optofluidic detection. We present a review on state-of-the-art optofluidic devices to quantify cellular phenotypes by using these optical techniques. The review summarizes the promises and limitations of each optofluidic scheme. Finally,

[a]*Research Center for Applied Sciences, Academia Sinica, 128 Sec. 2, Academia Rd. Nankang, Taipei, 11529, Taiwan*
[b]*Department of Mechanical Engineering, University of Michigan, MI, 48109, USA. E-mail: katsuo@umich.edu*
[c]*Institute of Biophotonics, National Yang-Ming University, Taipei, 11221, Taiwan*
[d]*Department of Physics, Southeast University, Nanjin, 211189, China*
[e]*Department of Physics and Materials Science, City University of Hong Kong, Tat Chee Ave. Kowloon, Hong Kong*
[f]*Department of Microelectronics, Fudan University, Shanghai, 2000433, China. E-mail: wenjunzhang@fudan.edu.cn*
[g]*Engineering Research Center for Wireless Integrated Microsensing and Systems (WIMS2), University of Michigan, Ann Arbor, MI, 48109, USA*
† Published as part of a themed issue on optofluidics.

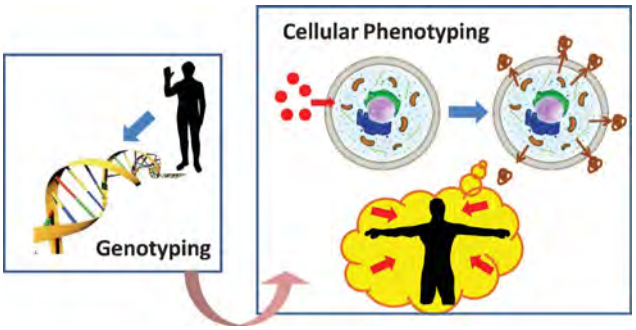

Fig. 1 Concept of genotyping and cellular phenotyping related to human health care. Genotyping determines the genetic program of human body that potentially triggers the onset of diseases. Cellular phenotyping provides important insights into the influence of both genetic programming and environment on human body and disease development by using an individual cell as a human biology model.

we discuss how the optofluidics research field may evolve to establish lab-on-a-chip technology advancing future cellular phenotyping studies.

2. Optical detection methods

Conventional optical detection methods are key enablers for cellular phenotyping measurements. Cellular phenotypes are generally divided into three categories: (1) nuclear-based phenotypes, (2) cytoplasmic phenotypes, and (3) functional phenotypes. Nuclear-level phenotypes include levels of gene expression, epigenetic modifications and protein binding to DNA and/or chromatin.[12] Cytoplasmic phenotypes are quantities of molecules (*e.g.*, protein) that stem from genetic codes or certain metabolites or by-products that result from cell signaling or biochemical cascades.[12] Functional phenotypes are defined with respect to cellular behavior in growth and proliferation and cellular immune response (*e.g.* cytokine secretion) or resistance to external stimulants, such as drugs and cytotoxic chemical substances. It should be noted that this categorization is not necessarily distinct as these phenotypes are often cross-linked.

This section provides an overview of four optical methods relevant to cell-type differentiation and briefly summarizes general optical integration schemes that have been developed.

2.1. Fluorescence detection

Fluorescence is the photoemission phenomenon of specific molecules when they absorb photons or other electromagnetic energy.[17,18] These molecules, usually called fluorophores or fluorescent dyes, are used as indicators for particular biomolecular visualization, environmental condition monitoring or cellular stimulation studies. Fluorescence detection is the most widely employed sensing technique for chemical or biological analysis. The technique benefits from well-established, highly sensitive, selective fluorescent labeling biomarkers and has ready access to a wide spectrum of commercially available fluorescence detection instruments, such as optical microscopes, multiwell plate readers, and flow cytometers. The general fluorescent-based detection systems usually consists of excitation light sources, such as lasers, light-emitting diodes (LEDs) and mercury lamps, sample holders, such as glass slides, multiwell plates or cuvettes, where a fluorescence-emitting process takes place, detectors, such as charge-coupled detectors (CCDs), photomultiplier tubes (PMTs), or spectrometers, to collect the emission signal and translate it into a microscopic image or electrical output.

One problem of using fluorescence detection methods is the auto-fluorescence of polymer materials or biomolecules, which gives rise to background noises and reduces the signal-to-noise ratio. Therefore, it is important to carefully select appropriate device materials and purified samples. Additionally, typical fluorescent probes have fairly a broad emission spectrum with full width at half maximum (FWHM) = 50–100 nm, which limits the total number of parameters reported with a fixed detection wavelength bandwidth. Moreover, the fluorescent labeling method usually requires complicated reagent manipulation processes (*e.g.*, vortex, centrifuge and filter) and a prolonged incubation time, which may affect the phenotype of target cells. Finally, the photo-bleaching effect of fluorescent probes makes long term cell-based assay monitoring difficult.

There are many commercially available fluorescent probes specifically for cellular phenotyping detection. For example, fluorescent proteins, such as green fluorescent protein (GFP), have been widely used as a probe to visualize, track and quantify protein translocation or its amount in living cells.[19] Other fluorescent probes target intracellular messengers of signal transduction, such as calcium ions (Ca^{2+}), pH, oxygen and CO_2. The change of these parameters allow researchers to understand how cells regulate different biological processes, including gene expression, metabolism, and apoptosis.[20] Another cellular phenotype that current fluorescent probes report on is cell immunity. It evaluates the condition of immune cells in response to outside invasion, such as bacteria or viruses. The immunofluorescence (IF) labeling technique has been widely used for monitoring the cellular immune status. Typically, the technique utilizes the specificity of fluorescent-labeled antibodies to target cells secreting a specific antigen or protein. The fluorescent image is then observed by a wide-field microscope. Flow cytometry and enzyme-linked immunosorbent spot (ELISpot) assay are the two most common technologies for single immune cell analysis.[21,22]

Fluorescence-based cellular phenotyping detection benefits from microfluidics that provides sample-efficient, high-throughput, and precise cellular environment control.[23,24] The optofluidic approach of merging optics with microfluidics further provides unique advantages that off-chip optics cannot accomplish. This approach provides higher sensitivity, multiplexity and multiple functionalities for chemical or biological analysis by integrating optical components into fluidics. For example, Balslev *et al.*[25] developed an monolithic hybrid optofluidic system to achieve on-chip sample mixing and detection. Tung *et al.*[26] embedded four optical fibers into a microfluidic flow cytometry device to achieve simultaneous two-color excitation/emission detection. Seo and Lee[27] developed a compound 2D microlens for focusing LED excitation light onto a microchannel region. Other groups integrated a light source[28] and a chip-size wavelength detector[29] towards realizing all-in-one system integration. The optofluidic integration enables development of a miniaturized and easy-to-use optofluidic platform for point-of-care (POC) diagnosis. Such a system permits simplified optical

alignment with cost-efficient and minimum optical components. However, a POC optofluidic system usually shows compromised sensing performance as compared to a highly sophisticated off-chip fluorescence microscopy system.

2.2. Surface enhanced Raman spectroscopy (SERS)

Raman scattering is a fundamental form of molecular spectroscopy, which refers to the phenomenon that involves excitation of a molecule by inelastic scattering of a photon.[30] Raman scattering is used to obtain information about the structure and properties of molecules from their vibrational transitions as well. Raman scattering is a two-photon event rather than one-photon event.[31] As the molecules are irradiated by the incident light, the incident photons may be absorbed or scattered or passed straight through. If the energy of a photon does not correspond to the energy gap between the ground state and an excited state of a molecule, the scattering of a photon can occur and produces Rayleigh scattering and Raman scattering. Rayleigh scattering, also called elastic scattering, corresponds to light scattered at the frequency of the incident radiation without energy loss; whereas the Raman scattering is an inelastic scattering and shifted in frequency which means the incident radiation by the vibrational energy is lost or gained in the molecule. The associated incident photon and the scattered photon are connected by a simple quantum mechanical process and makes Raman scattering a coherent two-photon event, which differs to the one-photon event of photon absorption after emission.[32] The typical Raman spectroscopy setup requires advanced laser technology coupled with high efficiency filters to suppress the scattered Rayleigh light and extremely sensitive detectors.[33]

The advantages of Raman spectroscopy are its versatility and high specificity, which could be applied to any optically accessible sample without a sample pre-treatment and finish a non-destructive measurement. However, the poor sensitivity of Raman spectroscopy caused by the low efficiency of the inelastic scattering processes has hampered its utility for a long time. Surface-Enhanced Raman scattering (SERS) is one promising approach to overcome this limitation.[34] A molecule situated in the vicinity of nanoscale metallic structures experiences dramatic enhancement of Raman scattering with more than a million-fold signal increase.[34] Today, there are two mechanisms generally agreed to produce the SERS effect: electromagnetic enhancement and the chemical charge transfer effect. In the chemical enhancement mechanism, the molecule chemically bonds to the metal and the excitation is through the transfer of electrons from the metal to the molecule and back to the metal again.[35] In the electromagnetic enhancement mechanism, the metal surface irradiated by a laser beam couples with the electromagnetic radiation.[36] The oscillations of the conduction band electrons confined on the nanoscale metal surface, a process called localized surface plasmon resonance (LSPR), result in a larger number of scattered photons.[37,38]

Previous research has reported non-invasive measurements by *in vivo* SERS-based detection for tumor discovery and glucose monitoring.[39,40] Compared to fluorescence emission and infrared absorption spectroscopy detections, SERS based on nanoscale metallic nanostructures provides the advantages of higher sensitivity, surface specificity, and fluorescence quenching,[41] moreover, simultaneous detection of multiple analytes could be possible owing to the sharp spectral signals with the narrow FWHM value up to 1 nm. It has been shown that SERS-based optical detection facilitates cellular phenotyping studies. For example, Lee *et al.*[42] used SERS imaging to study normal HEK 293 cells and cancer cells that express PLCγ1, a protein molecule that is known to promote breast cancer metastasis (Fig. 2). This study conjugated rhodamine 6G (R6G)-adsorbed Au/Ag core-shell nanoparticles with anti-mouse IgG. These particles specifically bind to PLCγ1 antibodies of the cancer cell surface. The Au/Ag core-shell structure takes advantage of the long-term stability of the gold surface and the superior Raman signal enhancement by the silver core, which is 100-1000 times greater than gold. Imaging the SERS spectra from the Raman reporter (R6G) on the single cell provided the phenotype signature unique to the cancer cell. More recently, the same group developed DNA-conjugated nanoparticles specifically targeting CD24 and CD44 receptor biomarkers and characterized three different breast cancer cell lines from the SERS characteristics of these nanoparticles with high specificity.[43]

Although "optofluidics" refers to a class of optical systems synthesized with fluids,[13] it is more true that for SERS detection applications to date most optical components such as the light source, lenses, waveguides and sensors, remain off the chip. The advantage of SERS-microfluidic platforms is to simply integrate certain fluidic tasks on a chip for optimized SERS detection: with a continuous flow and homogeneous mixing between the analytes and metal nanoparticles in the channels, higher

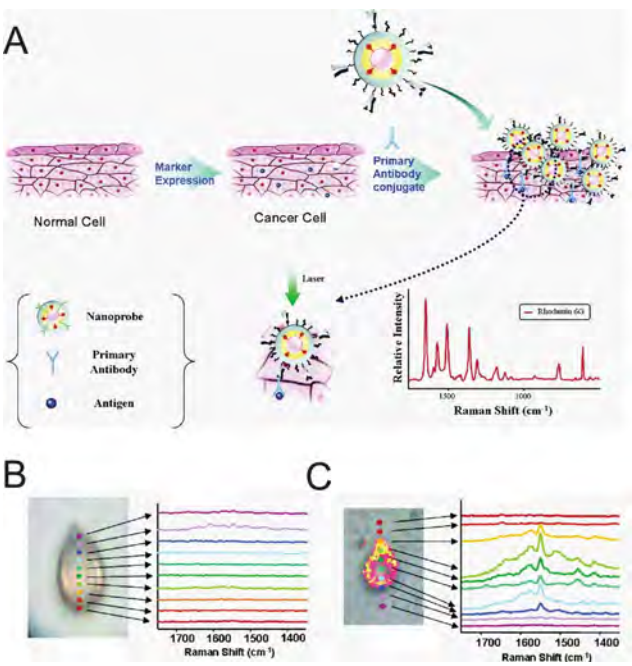

Fig. 2 (A) Immobilization of Au/Ag core-shell nanoprobes on PLCγ 1-expressing HEK293 cells and their SERS detection. (B) Spatial mapping of Raman spectra for single normal cell. Colorful spots indicate the probing spots across the middle of the cell along the vertical axis. (C) Spatial mapping of Raman spectra for single cancer cell. Colorful spots indicate the probing spots across the middle of the cell along the vertical axis. Reprinted from Ref. 42 with permission from American Chemical Society Publications.

reproducibility and stability can be attained. Furthermore, local sample heating can be prevented as molecules exposed to the laser are constantly refreshed due to fluid flow.[44] For more advanced applications, the synergistic integration of SERS detection and the microfluidic system into an optofluidic device should be considered: device integration combines optics and microfluidics on the same chip by building the optics from the same fluidic toolkit, and the optical properties of the SERS unit and analyte could be controlled by manipulating the fluids. The advantage of such an optofluidic system is to able be to carry out a series of optical measurements through fluidic controls and obtain reproducible enhancement factors for more reliable quantitative analysis.[16] Furthermore, ultra-sensitive SERS surfaces can be seamlessly integrated with micro/nanofluidic devices by fabrication techniques, such as soft lithography, to further improve the detection performance.[45]

2.3. Surface plasmon resonance (SPR)

A surface plasmon (SP) is an electromagnetic wave propagating along the surface of a metal/dielectric interface. Normally, SPs are formed when incident light coupled to a metal thin film by a prism undergoes total internal reflection. This condition also gives rise to the evanescence field, which is a near-field electromagnetic wave exponentially decaying into the dielectric medium opposite the prism. Surface plasmon resonance (SPR) arises when the photon frequency of incident light undergoing total internal reflection matches the natural frequency of the surface electron oscillation.[46] A strong photon-SP coupling during SPR causes absorption of the reflected light. SPR-based optical sensing techniques measure the absorbance spectrum, which is highly sensitive to the metallic surface condition determined by the refractive index of the dielectric medium. The techniques detect the surface binding of molecules on the metal surface by observing the resulting shift in the absorbance spectrum peak (or minimum) or the angle of reflection at the minimum intensity. SPR detection is often used for label-free chemical and biological sensing and permits high-sensitivity, real-time analysis. Moreover, SPR sensing is low cost so can be used for bio-diagnostics, food safety, environmental testing, *etc.*[47]

Recent advances in nanofabrication technology enable nanoscale modifications and nanoparticle coating of metallic surfaces. Current nanofabrication technology has made optical detection based on LSPR (see the SERS section) readily available for researchers.[38] LSPR-based detection measures shifts in the reflectivity (or alternatively, absorbance) spectrum of a nanostructured metal surface that is experiencing a condition change. The reflectivity spectrum can be spatially mapped across the surface to obtain a LSPR image. Although SPR has higher sensitivity than LSPR,[48] the LSPR technique provides advantages for measuring short-range changes in refractive index due to molecular adsorption. This is because the sensing volume is so small with LSPR. Furthermore, current nanofabrication technology is able to control nanoparticle shape and size for various materials, which permits tuning of the LSPR optical band ranging from the visible to the near-infrared region. We believe that integration of the LSPR sensing scheme in a lab-on-a-chip setting is more readily achievable than the SPR sensing scheme because of the simple optical configuration and sensing tunability.

SPR-based detection is generally used for cellular phenotyping studies. For example, Fang *et al.*[49] used a multi-gold-array biosensor to measure SPR spectra originating from a large group of leukemia CD33 cells. These cells were extracted from the human bone marrow of two patients using different sample preparation protocols. The technique detected shifts in the SPR spectra resulting from cells binding to antibody-immobilized gold sensing spots of the sensor surface. This sensor platform is cost effective, readily constructed, and easily handled in experimental settings. The analytical procedures are specific to the cell type and eliminate the labeling process. Without employing microfluidics technology, this research was not fully established for POC clinical use. However, it demonstrated that SPR detection is potentially useful for diagnostic detection of leukemia CD33 cells in the marrow aspirates of AML patients.

In the literature, we find several reports on SPR detection with a microfluidic or optofluidic chip for real-time monitoring of chemical and biological processes. Grasso *et al.*[50] used a Y-shaped microfluidic channel to mix two chemical (DSA: *Datura stramonium* agglutinin and AF: asialofetuin) solutions with great flow stability and achieved SPR signal mapping for regions of different degrees of mixing. A study by Chien *et al.*[51] presented advanced integration of three SPR waveguide channels, each having a metallic sensing patch, and light-focusing diffractive mirrors with a microfluidic channel (Fig. 3). The increased level of optical integration in this sensor could be suitable for microfluidic lab-on-a-chip applications. However, any practical use of the device was not demonstrated for parallel analysis of multiple biochemical compounds.

The LSPR technique using metal nanostructures has been demonstrated for label-free, real-time monitoring of biomolecular (not cellular) interactions within a microfluidic system. Huang *et al.*[52] developed a microfluidic chip with integrated LSPR biosensor–gold films and fluidic channels/chambers. The surfaces of the sensor films were coated with gold nanoparticles

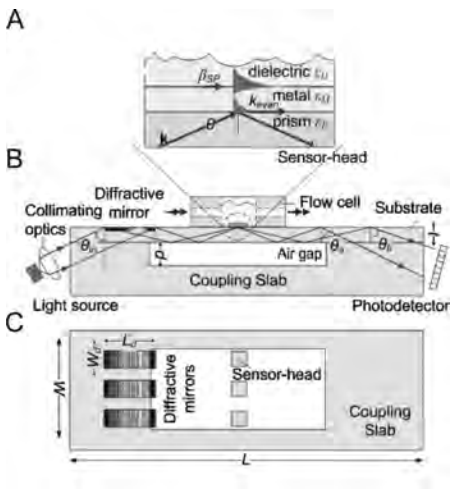

Fig. 3 Schematic of integrated three-channel SPR optofluidic sensor chip: (A) sensor head comprising a dielectric-metal-prism multilayer, where the incident light experiences total internal reflection, (B) cross-sectional view showing an integrated diffractive mirror that gives rise to various incident angles of light. (C) Top view showing three integrated diffractive mirrors and sensor heads. Reprinted from Ref. 51 with permission from Elsevier.

and subsequently biotinylated. With this optofluidic chip, the study demonstrated real-time monitoring of biotin/anti-biotin binding from the light transmission of the sensor films. More recently, Danz *et al.*[53] developed a disposable, injection-molded microfluidic chip incorporating one-dimensional SPR sensor arrays. Coupling this chip with an off-chip angular-resolved spectrometer, the researchers performed parallel detection of genetic variations among different DNA samples prepared by polymerase chain reaction (PCR). Malic *et al.*[54] achieved both enhanced sampling handling and increased sensitivity (limit of detection = 500 pM) for SPR-based DNA hybridization detection using total internal reflection. The research team integrated both a nanostructured gold sensor surface and a digital electrowetting micro-droplet manipulation mechanism on a microfluidic chip (Fig. 4). This study represents a synergistic combination of SPR detection with LSPR signal enhancement.

2.4. Interferometric detection

The general principle of an interferometer is based on photo detection of the interference pattern or intensity of two previously coherent optical waves passed through optical paths with unequal distances. The optical path difference can be due to either a difference in the physical distance length or a phase shift caused by a refractive index (RI) change of the waveguide media. The latter case is more relevant to biological and chemical sensing. Both the Mach-Zhehnder (M-Z) and Michelson interferometers[55] use a beamsplitter to split a wave from a laser light source into two waves, another (or an identical) beamsplitter to recombine them following their passage of the unequal distance paths, and a CCD imager or photomultiplier tube (PMT) to obtain the interference pattern and intensity. The basic setup of the Fabry-Perot (F-P) interferometer (or cavity)[55] consists of a cavity between two partially reflecting flat surfaces parallel to each other. A wave from a light source is collimated by a lens and passed through the cavity. Interference occurs between the multiple reflections of light between the two surfaces. The transmission spectrum has a high peak corresponding to constructive interference of in-phase transmitted beams and a minimum corresponding to destructive interference of out-of-phase transmitted beams. A focusing lens collects the transmitted beams, and a photodetector (*e.g.*, photodiode and photoelectric device) detects the interference intensity. The transmission spectrum varies with the cavity distance and the RI of a homogeneous medium inside the cavity.

Similar to SPR-based methods, interferometric detection permits label-free biological and chemical sensing. This eliminates the use of signal-reporting molecules such as fluorophores, dye chemicals, quantum dots, and nanoparticles that may be potentially harmful to living organisms. This technique is noninvasive to tissue and cells, using light in the near-infrared and infrared wavelength regions between 600 and 1200 nm. This wavelength band is called "therapeutic zone for laser treatment," where human tissue and cells have low light absorption.[9] The measurement obtaining RI information from biological cells is remarkably sensitive and repeatable. This makes refractometry enabled by interferometric detection highly suitable for use in identification of cells with great selectivity. One of the significant challenges facing this technique is that it is extremely susceptible to slight disturbance in the environment such as moving or shaking when using free-space optics. The operator needs much care in handling the movements of the living cell and surrounding buffer to avoid disturbances. This makes the integrated optofluidic approach highly viable for advancing interferometric detection as shown later.

The effective RI is a good indicator of the constituents of a living cell, such as its membrane, organelles, cytoskeleton, cytosol, nucleic acids, and protein contents. Changes in cell size, cell mass, nuclear size, and nuclear content can be indications of changes in cells, such as onset of disease, for example, cancer. It has been shown that these biophysical changes translate to a shift in the overall refractive index of the cell.[56] For example, diseases such as iron deficiency anaemia or thalassemia, cause abnormalities in the haemoglobin content in a red blood cell. This will result in a deviation in the RI of cell. High levels of protein content exist in cancerous cells for their adaptation to rapid cell proliferations,[10,57] which cause higher RI than the normal cell exhibits.

Ultimately, optofluidic technology could potentially achieve monolithic optics-fluid integration for interferometric detection.

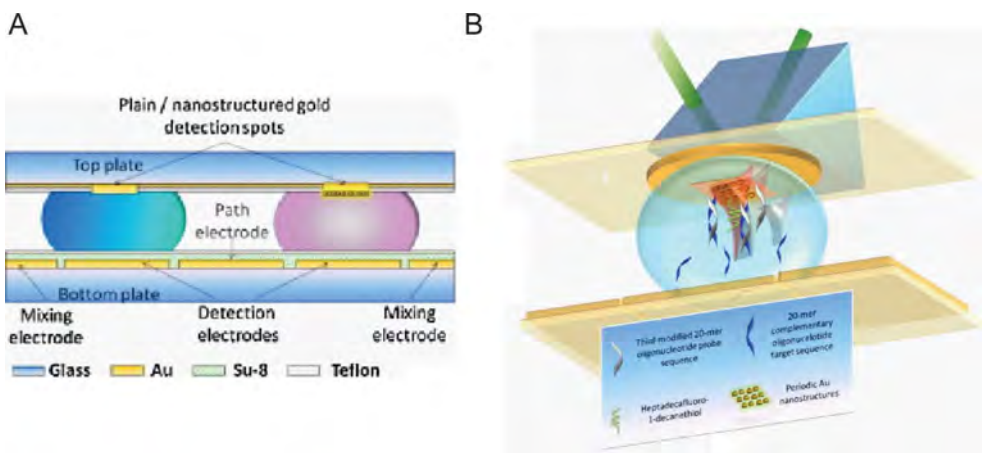

Fig. 4 Schematic of electrowetting on dielectric (EWOD)-SPR optofluidic chip: (A) vertical cross-section showing reagent microdroplets manipulated on a dielectric layer. The hydrophobicity of the dielectric layer is controlled by changing the voltage applied to the embedded electrodes. (B) Illustration of SPR detection-based assay of DNA hybridization using EWOD droplet manipulation. Reprinted from Ref. 54 with permission from Elsevier.

As we see for the other detection techniques, current studies are yet to achieve a fully integrated interferometric microsystem, only limiting their work to partial integration of interferometer components. The technological benefit of the optics-fluid integration is particularly great for this technique. Research in this field has established the ability to integrate planar waveguides in a microfluidic system.[14] Such on-chip waveguides are suitable to construct highly compact integrated optofluidic interferometric architectures with Y-waveguide junctions.[58,59] The use of optofluidic interferometers provides improved light-liquid interaction with their integrated optical components[58] for interferometric detection as well. The precise on-chip placement of optical fibers and beamsplitter lens with respect to a microfluidic interrogation region enables manual alignment-free optical probing of a liquid sample.[60] For example, Domachuk *et al.*[61] constructed a highly compact optofluidic F-P interferometer with a cavity precisely formed between optical fiber Bragg grating reflectors across a planar microfluidic channel. They carefully positioned the phase reflection plane of Bragg reflectors several periods out of the fiber surfaces. As a result, the effective cavity length became substantially longer than the channel width, which reduced the sensitivity to cellular IR. Using the device, the researchers successfully detected index changes as low as 0.2% for aqueous sodium chloride solution at varying concentration.

Additional integration of fluidic/mechanical actuators and mechanically deformable structures further enables reconfigurable microfluidic interferometry. One such example is an optofluidic Michelson interferometer by Chin *et al.*[62] that incorporates a Bragg liquid-core waveguide with its grating period varied by a droplet plug flow (Fig. 5). This device measured a variation in the refractive index of glycerol solution at different concentrations. Another example is an optofluidic interferometer pressure sensor demonstrated by Song and Psaltis[63] using an air-gap optical cavity embedded next to a membrane of the microfluidic channel wall. The membrane deflection changed the cavity size, changing the optical path length. Imaging the interference patterns of waves reflected by the top and bottom cavity surfaces allowed the researchers to measure the pressure for the microchannel flow at a large dynamic range.

For general biomoelcular detection, several studies demonstrated label-free binding immunoassay using optofluidic interfeormetry.[15,16,64] Biochips used in these studies typically incorporate two split on-chip waveguides, one of which has an antibody-functionalized surface area that serves as an active sensing region. The binding of analyte molecules onto the sensing region causes a change in the refractive index along the optical path. The resulting interference pattern or intensity variation determines the analyte concentration in a biological liquid sample.

3. Optofluidic devices for cellular phenotyping

In the next few years, we expect the research community to see a rapid increase in effort towards development of optofluidic technology for cellular phenotyping based on the optical detection methods described above. This section reviews recent reports on microsystems integrating optics with a microfluidic platform and summarizes how they facilitated cellular phenotyping measurements. Table 1 summarizes the studies reviewed in this section.

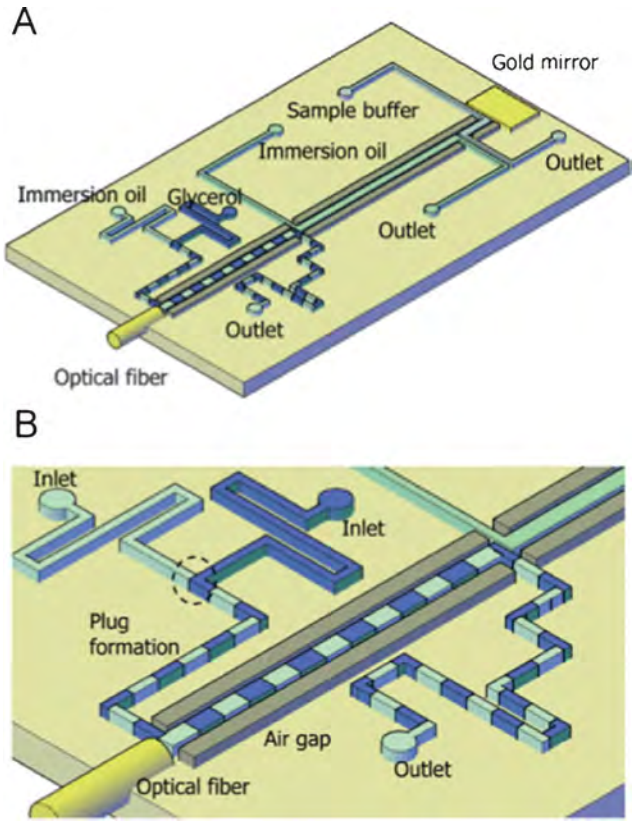

Fig. 5 (A) Schematic of a reconfigurable optofluidic Michelson interferometer incorporating a Bragg liquid-core waveguide. (B) A droplet grating is formed by on-chip fluidic actuation. This microfluidic waveguide design employs the droplet grating in the microchannel as a core layer. The transmission spectrum of light passing through the waveguide provides changes with the droplet period and permits the refractive index measurement of the sample buffer. Reprinted from Ref. 62 with permission from the Royal Society of Chemistry.

3.1. Fluorescence detection-based optofluidic devices

We find many studies that focus on developing optofluidic flow cytometers in a simplified, cost-effective, and disposable chip platform for fluorescence detection-based POC cellular analysis. Frankowski *et al.*[65] demonstrated a microfluidic flow cytometer to achieve immunological differentiation of leukocyte subpopulations (*e.g.*, lymphocyte, monocyte, and granulocyte) using fluorescently-labeled CD3, CD4, CD14, and C45 surface biomarkers. With its carefully designed microfluidic structure, the device permitted two-dimensional sample focusing by only one sheath flow. In this device, an optical fiber embedded in close proximity to a microfluidic channel enabled high-sensitivity detection. The device can potentially be used for immune cell counting for HIV or other disease diagnoses with small sample volumes. However, the entire system still required multiple off-chip emission filters, dichoric mirrors, and PMTs to achieve multi-color fluorescence detection. As a result, the whole system remained bulky and its operation would still require tedious manual optical alignment with high precision as conventional flow cytometry does.

Huang *et al.*[66] developed a new optofluidic flow cytometry technique so called "microfluidic multispectral flow cytometry (MMFC)" with much simpler optics. The technique only

Table 1 Summary of cellular phenotyping optofluidic devices

Detection scheme	Integrated on-chip optical components	Cell type	Phenotype	Clinical/biological relevance	Specificity[a]	Reference
Fluorescence	Embedded fiber, mirror	Leukocytes	Surface biomarkers	HIV	High	Frankowski *et al.*[65]
Fluorescence	Embedded fiber	HeyA8 epithelial tumor cells	Protein abundance/ cell viability	Gene expression, intercellular Ca^{2+}	High	Huang *et al.*[66]
Fluorescence	Microlens, optical tweezers	Yeast cells	Intracellular pH	Metabolism and cell growth	Medium	Werner *et al.*[67]
Fluorescence	Off-chip optics only	B lymphocytes	Protein translocation	Cancer treatment	N/A	Wang *et al.*[68]
Fluorescence	Focusing lens	Yeast cells	Cellular viability	Cell counting	N/A	Rosenauer *et al.*[71]
Fluorescence	Emission filter	CD4 lymphocytes/ CD4 monocytes	Surface biomarker/ cell size	HIV	Medium	Kiesel *et al.*[72]
Fluorescence	Waveguide	L929 mouse fibroblasts	Cellular morphology	Cell counting/ binding kinetic	N/A	Schelb *et al.*[74]
Fluorescence	Light source, focusing lens, filter, camera	White blood cells	Surface biomarker	HIV	High	Zhu *et al.*[75]
Fluorescence	Off-chip optics only	THP-1 monocytes	Cellular immunity	Immune/infection disease	High	Ma *et al.*[76]
SERS	Off-chip optics only	CHO (Chinese hamster ovary) cells	Cellular chemical dynamic response	Nucleic acids, proteins, lipids, carbohydrates, intercellular Ca^{2+}	N/A	Zhang *et al.*[82]
SERS	Off-chip optics only	*E. Coli*	Cellular wall components/ cytoplasm information	Bacteria identification	High	Walter *et al.*[83]
SPR	Antibody-immobilized optical sensor array	CD4+ T cells	Cellular immunity	Autoimmune disease	High	Rice *et al.*[84]
Interferometry	Fabry-Perot resonant cavity	HSA (hemangiosarcoma) cells/monocytes	Intracellular protein content	Canine cancer	High	Wang *et al.*[88]
Interferometry	External cavity laser, microlens, mirror	Human astrocytes cell/glioblastoma cells	Intracellular protein content	Brain tumor	High	Liang *et al.*[10]

[a] "High" – measurements yielding a p-value <0.01 for two cell populations of different phenotypes; "Medium" – measurements permitting qualitative cellular phenotype differentiation from data mapping; "N/A" – no statistical data or histograms available.

required the use of a single laser and a single PMT detector for flow cytometry with multiple label colors (Fig. 6). The researchers integrated a spectrometer unit consisting of a strain-tunable nanoimprinted grating microdevice chip and the PMT with a microfluidic channel *via* an embedded optical fiber waveguide. The system permitted high-speed (>1 kHz) continuous photospectrum acquisition for multiple fluorescence-emitting cells flowing in a microfluidic channel. The MMFC technique spectrally identified fluorescence signals from a HeyA8 epithelial tumor cell line transduced with green fluorescent protein (GFP) and from the same cell line stained with calcein-AM (cell viability kit). These two fluorescent probes have highly

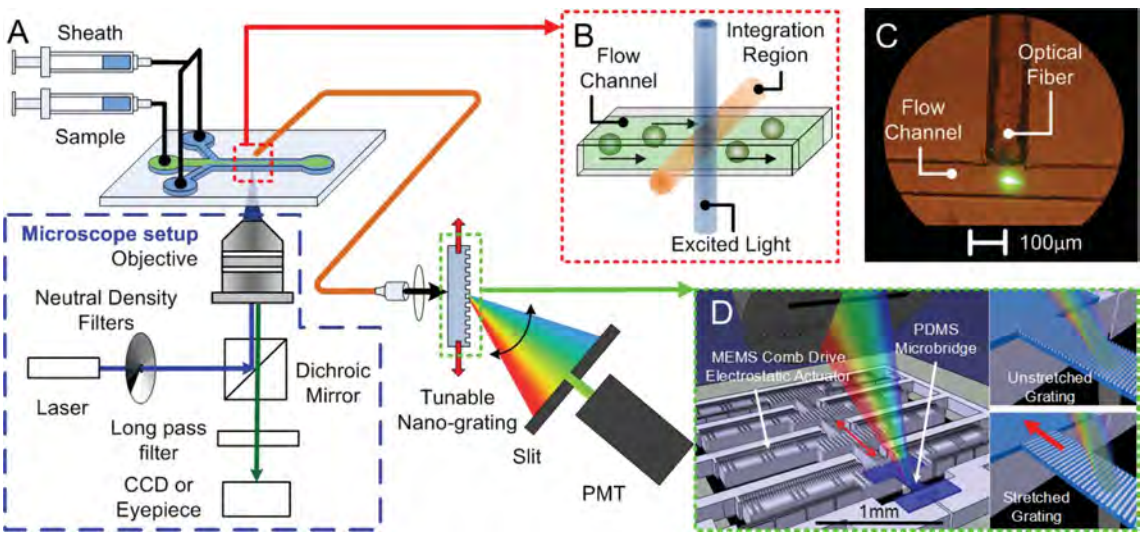

Fig. 6 A) Microfluidic multispectral flow cytometry (MMFC) setup. (B) Fluorescent particles pass through the channel's interrogation region. (C) A fluorescently-labeled single cell is excited at the interrogation region. (D) Working principle of the tunable grating microdevice. The collected light is dispersed through the transparent elastomeric grating. The mechanically soft grating is repeatedly stretched by on-chip silicon microactuators to achieve real-time single-detector spectroscopy of fluorescent emission signals. Reprintedfrom Ref. 66 with permission from the American Chemical Society Publications.

overlapping spectra with a peak-to-peak wavelength difference <5 nm, which the conventional multicolor flow cytometry system cannot resolve. The demonstrated spectrum resolving power promises to enable cellular gene expression discrimination with a larger number of combinations of fluorescence proteins with similar emission spectra (*e.g.*, CFP/GFP and GFP/YFP) and to permit measurements of cellular protein abundance and intercellular Ca^{2+} concentration at higher accuracy.

The ability to manipulate individual cells has been achieved with integrated optics for optofluidic fluorescence detection. For example, Werner *et al.*[67] demonstrated a microfluidic flow cytometer array integrated with microlens-focused optical tweezers to trap and sort over 200 yeast cells. The researchers used this system to investigate a variation in the intercellular pH values of cells exposed to extracellular glucose, which indicate their physiological regulation level. The drawback of this technique was the spatial non-uniformity of the optical force from cell to cell. This adversely affected the measurement accuracy and throughput.

Wang *et al.*[68] used a two-layer microfluidic structure to achieve on-chip single cell fixation for total internal reflection fluorescent (TIRF) measurement (Fig. 7). In this device, an integrated pneumatic microactuator repeatedly trapped flowing individual cells and fixed them against a channel wall surface emitting the evanescent field. The evanescent excitation locally excited the fluorescent dye of the cell within ~100 nm from the substrate surface. The technique probed the cell's protein translocation, which is an important cellular phenotype indicating the therapeutic outcome of cancer and other diseases.[69,70] The coupling of TIRF with flow cytometry is uniquely enabled by the optofluidic approach. This could be further extended to achieve a rapid and precise observation of the cytosol-to-nucleus translocation of a single cell.

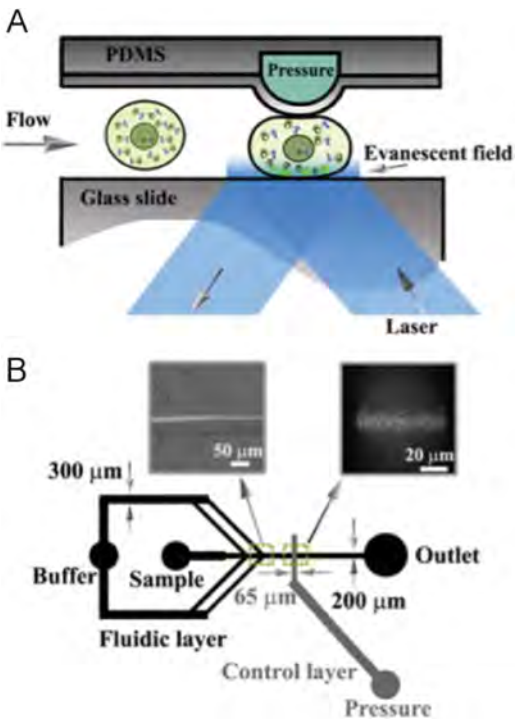

Fig. 7 (A) Schematic of microfluidic TIRF-FC device integrating an elastomeric valve that forces flowing cells into the evanescent field near the surface of the microfluidic glass channel wall. (B) Top view showing the hydrodynamic focusing and TIRF fluorescence image of cells. Reprinted from Ref. 68 the permission from the Royal Society of Chemistry.

Significant advances in point-of-care (POC) optofluidic cytometry can be found in recent literature. Rosenauer *et al.*[71] used an adjustable fluidic lens with three dimensional focusing to count the viability of methylene blue-stained yeast cells. Kiesel *et al.*[72] demonstrated a microfluidic flow cytometer monolithically integrating a photodetector chip, a filter, and a spatially patterned mask (Fig. 8). The mask modulates the fluorescent emission propagating toward the detector. The resulting time-domain modulation of the detector signal provides information on both the emission intensity and flow speed of single-profile cells. The researchers showed that the two measured parameters and their combination serve as indicators of the sizes of the detected cells. The technique quantitatively obtained the counts of human CD4+ lymphocyte and CD4+ monocyte cells by detecting the fluorescent intensity from labeled CD4 surface biomarkers. They also used a flow speed-intensity mapping plot to differentiate the cell types based on their sizes. This study is notable in that it provides a new cell-type identification modality for POC flow cytometric measurement.

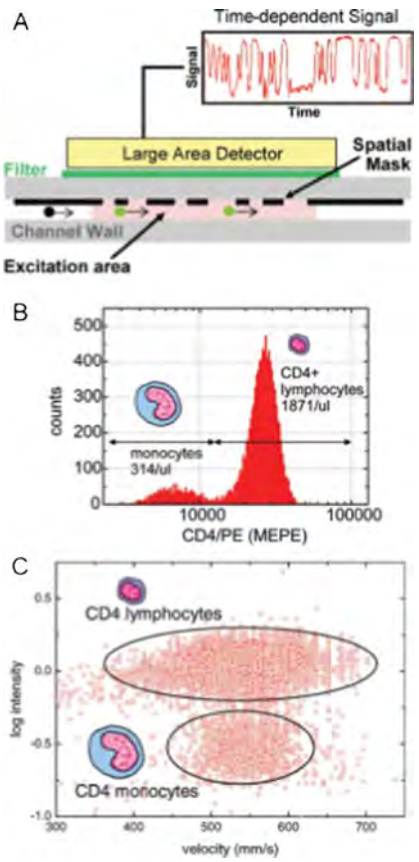

Fig. 8 (a) Schematic cross-sectional diagram of fluidic channel illustrating the concept of spatially modulated emission. Correlation techniques are applied to determine the position of the particle in real time. (b) Histograms of detected CD4 cells as a function of fluorescent intensity. This illustrates a CD4 count in whole blood. (c) Fluorescence intensity as a function of speed for CD4 cells. Compared to the CD4 lymphocytes, the larger CD4 monocytes show a narrower speed distribution as the flow focusing constrains them to a narrower range in the flow profile. Reprinted from Ref. 73 with permission from Wiley.

There are more optic-fluid integration examples for POC cytometry. Schelb *et al.*[74] monolithically integrated a polymer waveguide with a microfluidic channel to excite flowing cells only located on the tip of the waveguide by the evanescent field. The demonstrated ease of handling waveguide-cell alignment in the microfluidic channel may open a way for advancing POC technology. Zhu *et al.*[75] demonstrated a very unique approach to monolithically integrated optofluidic micro-cytometery by developing a cell phone based fluorescent imaging micro-cytometer. They assembled two LED light sources, a lens, and a plastic color filter all together on a cell phone CMOS camera. With the cost-efficient components that require minimum optical alignment, they successfully achieved counting of SYTO16 nucleic-stained white blood cells with a good correlation to commercial hematology analyzers.

A multiplexed cellular phenotyping assay done by Ma *et al.*[76] shows impressive throughput resulting from the use of a highly integrated microfluidic circuit. They constructed a two-layer PDMS microfluidic network consisting of 1040 nL microchambers for single cell confinement, each having a top layer with integrated vertical valves and a bottom layer with a microchannel (Fig. 9) Primary antibodies were immobilized on the chip substrate following a protocol similar to that of ELISpot assay, which is a common method for quantitative multiplexed analysis of cell-secreted cytokine panels. The platform was used to compare the polycytokine production of healthy CD3+ CD8+ T cells against that of melanoma-associated antigen specified CD3+ T cells. This study successfully demonstrated the advantage of microfluidic technology in acquiring large biological datasets with off-chip optics and spatially mapped fluorescence signals across the chip. This approach has proved very powerful in cellular phenotyping detection, evidenced by the rapidly increasing number of related studies in recent literature.[77–81] In fact, these studies make us re-evaluate efforts by the optofluidics research community towards on-chip optics integration targeting POC applications. We see that any advances in optical detection to facilitate laboratory-level assays are also highly valued by the life sciences research community whether they use on-chip or off-chip optics.

3.2. SERS-based optofluidic devices

The practical use of SERS for cellular phenotyping is still challenging as it requires tedious sample manipulation and sophisticated instrumentation. Together with microfluidics, optofluidic SERS-based cellular phenotyping platforms have the potential to improve the utility of the SERS effect in practical applications. We find significant progress has been made in the integration of detection optics into a microfluidic device to simplify the operation and to further enhance the detection performance for SERS measurements. However, it is generally

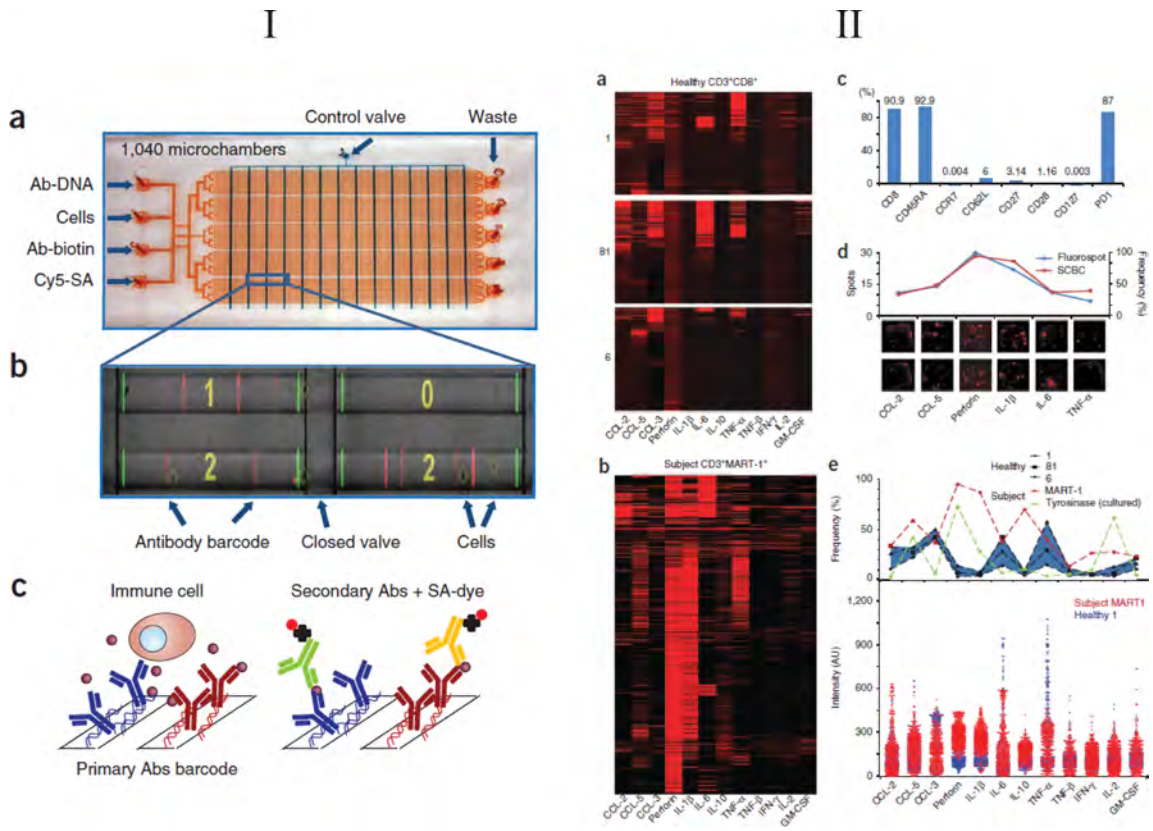

Fig. 9 (I) Schematic of single-cell barcode chip for cell secreted polycytokine analysis. (a) Photograph of two-layer PDMS microfluidic for single cell confinement. (b) The optical micrograph shows the isolated cells in each microchamber overlaid with the fluorescent antibody barcode. (c) Working principle of how cell-secreted antigens attach to primary antibodies and become sandwiched to bind to secondary antibodies conjugated by fluorescent dye for detection. (II) Comparison of polycytokine level between healthy CD3+ CD8+ T cells and melanoma-associated antigen apecific CD3+ T cells. Reprinted from Ref. 76 with permission from the Nature Publishing Group.

true that these optics-integrated platforms are not applied for cellular phenotyping. Current cellular phenotyping studies using SERS-based optofluidic device still focus on sample manipulation to precisely monitoring intracellular contents.

For example, Zhang *et al.*[82] studied the chemical dynamics inside a living cell by SERS with an improved sample handling capability within a microfluidic channel. The researchers demonstrated integration of a wide range of technologies including microfluidics, surface-enhanced Raman scattering, and confocal micro spectroscopy. This approach permitted *in situ* characterization of single living CHO (Chinese hamster ovary) cells with a high degree of spatial (in three dimensions) and temporal (1 s per spectrum acquisition) resolution. This study introduced gold nanoparticles of 50 nm in diameter into the cells by passive uptake to enhance the Raman signals. Furthermore, the study developed a Y-shaped (two inlets, and one outlet) microfluidic network to investigate the dynamic response of the cells. The assay delivered the cell suspension from one inlet of a microfluidic chip, while test solutions were introduced from another inlet for better control of chemicals in the temporal domain. With this setup, the researchers successfully measured the real-time Raman spectral signatures from the cells undergoing the agonist-evoked Ca^{2+} flux process induced by their exposure to a continuous flow of ionomycin.

Another example is a fast, highly specific and reliable bacteria detection platform by Walter *et al.*[83] The study developed a SERS-based microfluidic system to enable generation of reproducible and specific Raman spectral signature patterns as well as establishment of large databases for statistical analysis. In this work, the SERS spectra were taken from ultrasonically burst bacteria. The spectral signatures were used to probe phenotype information originating from the cell wall as well as the bacterial interior. The researchers used a microfluidic device equipped with 4 inlets (Fig. 10). The assay introduced a mineral oil separation medium, potassium chloride solution, silver colloid particles, and a bacterial suspension into the microfluidic chip. The aqueous analyte/colloid solution formed droplets within the mineral oil medium, consequently creating a segmented flow. This flow prevented deposition of nanoparticles and analyte on the microfluidic channel wall. The nanoparticles can either be coated

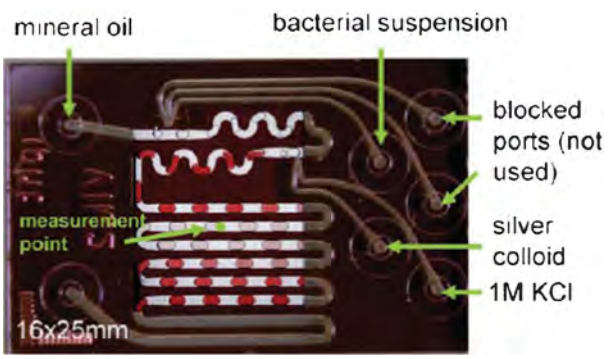

Fig. 10 Microfluidic chip with 6 injection ports (4 used, 2 blocked) that applies two phase liquid/liquid segmented flow. The two phase liquid/liquid segments constantly flow during the measurements. Raman spectra of the separation medium oil and SERS spectra within the droplets are detected at the measurement point in the second channel. Reprinted from Ref. 83 with permission from the Royal Society of Chemistry.

outside the bacterial cell wall or introduced to the interior of the bacterial cells for SERS signal enhancement. The enhanced signal intensity reduced the spectral recording time to 1 s. With this method, the researchers established a database of 11 200 spectra for a model system for *E. coli* including nine different strains.

3.3. SPR-based optofluidic devices

We have seen that optofluidic technology is well developed for label-free SPR/LSPR detection of DNA and protein molecules. However, our literature survey finds a relatively small number of studies aimed at optofluidic cellular phenotyping. In one of such studies, Rice *et al.*[84] constructed an optofluidic device for differentiation of CD4+ T cell subsets. The device was built on a microarray platform that permits both surface plasmon resonance imaging and surface plasmon coupled emission (SPCE) fluorescence detection by the photon-grating coupling principle. The researchers assessed the functional phenotype of the T cell subsets from their cytokine secretion levels. The cells were bound to the surfaces of the device's sensor pattern arrays, where both the cell-capture ligands and the anti-cytokine antibodies were co-immobilized. The study found that the T cell cytokine secretion pattern can be a good prognostic indicator of autoimmune disease and therapy. The SPR-fluorescence dual-modality approach may find broad use in the early diagnosis of T cell-mediated diseases. The optofluidic assay could provide rapid, high-content T cell screening data.

3.4. Interferometry-based optofluidic devices

Interferometry-based cellular phenotyping highly benefits from the optofluidic approach. Recent studies demonstrated differentiation of cell types by measuring variations in their optical properties using optofluidic F-P interferometers. A common approach among these studies involves (1) placing individual cells in a resonant cavity between two opposing fibers or in a cavity external to laser and (2) observing cavity mode modifications by the presence of cells. Precise holding of individual cells inside the cavity by conventional micropipette manipulations is cumbersome and difficult to achieve. As a result, it is not until recently that interferometric optical detection has become more readily available for single cell study. Recent advances by optofluidic research have brought about the ability to precisely manipulate the position of a single cell in a fluidic environment.

An example of optofluidic single cell refractometry is the Fabry-Perot cavity interferometer device demonstrated by Song *et al.*[85] (Fig. 11A). Their optofluidic device consists of a passive horizontal cavity between gold-coated single-mode fibers on opposite microfluidic channel walls and a cell-holding micropipette integrated orthogonal to a microfluidic channel. The measurement was performed for the Madin Darby canine kidney (MDCK) cell, a type of kidney cancer cell, with 0.1% accuracy. More recently, the same group extended this approach to achieve on-chip single cell refractometry based on optical cell trapping and M-Z interferometry. The new device design enabled them to measure the weight of the total substance other than water inside the living cell with improved repeatability and stability.[86] However, these measurements rather focused on cellular refractometry itself and need to prove themselves to be useful for practical cellular phenotyping.

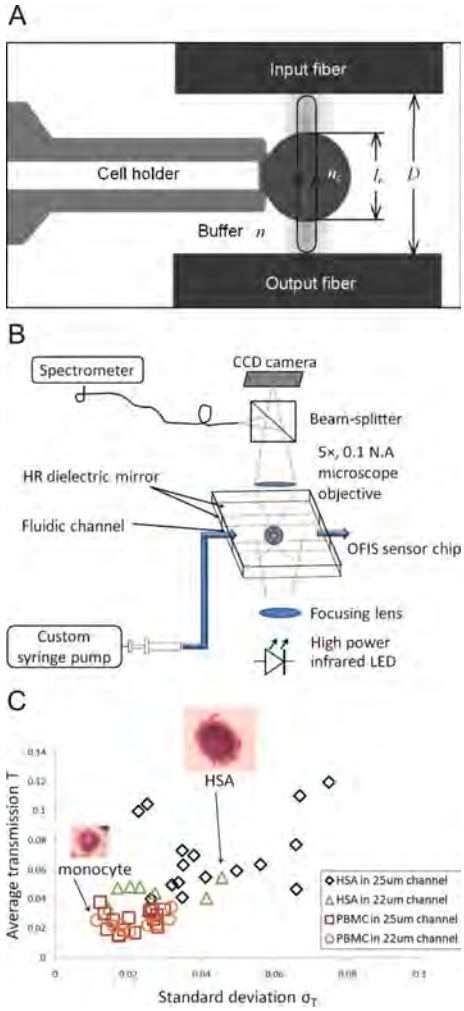

Fig. 11 (A) Schematic of a microfluidic Fabry-Perot (F-P) resonant cavity for cell detection by Song *et al.* in Ref. 85. A single cell is trapped within the cavity using an integrated micropipette holder. (B) Setup for label-free optofluidic spectroscopy using a microfluidic F-P cavity. (C) Scatter plot of transmission results of HAS and monocyte cells. (B) and (C) reprinted from Ref. 88 with permission from BioMed Central.

Lear's group[87,88] conducted more in-depth differentiation of cell types by statistically characterizing the transmission spectra of a single-cell trapping F-P cavity (Fig. 11B). The cavity transmission mode is affected by both the cellular RI and size.[89] Their device has a microfluidic channel etched into a Pyrex substrate and a Pyrex layer bonded to the channel substrate. The Pyres cover surface facing the channel has a coating of reflectivity dielectric mirror. The channel and reflecting surface cover form a microfluidic optical cavity resonator. The researchers collected transmission spectra of cells with various channel depths. With this device, the researchers could distinguish hemangiosarcoma (HSA), which is an aggressive canine cancer cell line, and monocyte samples at a statistically high significance with $p = 10^{-6}$. (Fig. 11C) The same method also allowed them to tell a difference in the optical phenotype of canine lymphoma and lymphocytes with $p<0.005$. The statistical analysis of the transmission spectra proves that the intracavity spectroscopy is a powerful method to simultaneously obtain high sensitivity and specificity in differentiating neoplastic and nonneoplastic cells.

Prior to the aforementioned studies, Gourley *et al.*[9] first explored the intracavity spectroscopy of cells using a device called the "biocavity laser." The biocavity laser is a photo-pumped vertical-cavity surface-emitting laser (VCSEL) with a cell-holding external cavity. The cavity is formed by a microfluidic channel and serves as the semiconductor gain region. This technique measured the frequency shift and intensity modulation of the laser emission affected by the cellular light scattering property and RI. This optofluidic device quantified the protein content levels of human astrocytes (normal brain) and glioblastoma (brain tumor) cells in a different growth phase and the concentration of haemoglobin in the red blood cells.[9] The same technique differentiated the healthy and diseased states of human mitochondria from laser spectral images.[90,91] Furthermore, Liang *et al.*[10] reported an optofluidic microchip monolithically integrating a laser diode, a microlens, a mirror, and a microfluidic channel (Fig. 12A). Similar to the biocavity laser, the microfluidic channel between the reflective surface of the laser diode and the mirror forms a resonant cavity (Fig. 12B). Alterations of the laser emission spectrum provided the RI values of human cancer cells, such as HeLa (cervical cancer), MCF-7 (breast cancer), and Jurkat (CD4 T-cell leukemia) cells.

4. Outlook

Over the last 20 years, the field of genomics – a discipline to determine and map the entire DNA sequences of living organisms – has seen explosive advances.[92–96] Scientists have obtained some

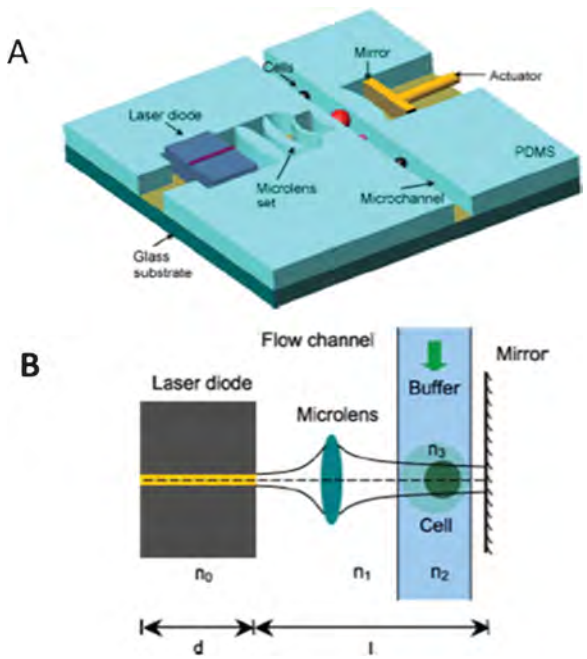

Fig. 12 (A) Schematic of monolithically integrated optofluidic external cavity laser chip. (B) Schematic of biolaser measurement with an external microfluidic channel cavity. A single cell is passed through laser light orthogonal to the microfluidic channel. The passage of the cell with a RI of n_3, which is different from the RI of the buffer n_2, causes laser emission modifications. Reprinted from Ref. 10 with permission from ScienceDirect.

insight into the mechanism of life through genomics. Modern life sciences still see further challenges towards translating the discoveries in genomics into a full understanding of genetically- and environmentally-affected human traits and disease developments. Statistical noise in genomic data often makes it difficult to elucidate the cause of underscore biological effects.[11,12] Modern biology has come to recognize that heterogeneity in non-genetic cellular phenotypes is one of the key factors governing core processes that occur at the cellular level, including proliferation, stimulus response, carcinogenesis, and drug resistance. Many diseases, including cancer, originate in a single or a few cells showing abnormal phenotypes. Early detection of the onset of a cellular phenotype abnormality would allow better disease diagnosis and treatment. Optofluidics is an exciting research field, particularly during the current transitional period with biological research. Optofluidic technology holds great promise to serve as a powerful tool to enable single cell-level phenotype characterization. We strongly believe that the importance of this field will be more pronounced than ever as cellular phenotyping research manifests its need for advanced optical detection tools.

Optofluidic systems realize efficient, fast, skill-free on-chip operations in manipulation and handling of individual cells and assay reagent loading while securing optical access to on-chip samples. Here, we propose to extend the definition of ''optofluidics'' to broader systems capable of advancing microfluidics with optics. Future research can focus on advancing microfluidic cellular phenotyping techniques to the point that they become equipped with unprecedented levels of throughput.[76–81,97] Coupled with a massively parallel microfluidic single-cell manipulation platform, optical technologies leading to higher sensitivity, accuracy, and signal handling capability would generate a huge number of phenotype datasets and provide a higher degree of information. In the context of enabling cellular phenotyping assays, the effort to achieve monolithic optics-fluid integration perhaps does not find a great value. Here, an emphasis should be placed in performing sophisticated fluidic actuation for sample loading, transporting, and sorting with highly sensitive, selective optical detection done by using off-chip optical instruments. As found with current studies on SERS and LSPR,[34,37,38] signal enhancement by nanostructures integrated in a microfluidic channel will continue to be an important research topic. Along with this direction, researchers also need to note that optofluidic technology has the great potential to integrate multiple optical detection modalities (*e.g.*, fluorescence + SERS, fluorescence + SPR, fluorescence + interferometry) in a common microfluidic platform. Such a multi-modality detection approach may synergistically enable multi-parametric analyses with high sensitivity and specificity. Multi-parametric analysis devices are ''must-have'' tools for data-intensive genotype-phenotype mapping assays.

Of course, the research community can be directed towards another important direction, which focuses on developing fully integrated standalone micro-analytical devices for POC applications. We find a majority of the reviewed studies still requires the use of large, expensive, and sophisticated off-chip lasers, detectors, and spectrometers. As seen in semiconductor and microelectromechanical systems (MEMS) industry, system integration and packaging are a critically important research area to enable future mass production and commercialization. We expect to see this research field evolving to provide innovative monolithic optics-fluid integration schemes. We expect that growth towards this research direction, shown by the recent demonstration of fluidic channel-on-a-CCD detector chip,[98–100] spectrometer-on-a-fluidic chip,[29] and flow cytometer-on-a-cell phone[75] devices, will open ways for development of standalone cellular phenotyping microchips for global health care.

Acknowledgements

The authors acknowledge support by the National Science Foundation under grants CBET-0966723 (K.K.) and ECCS-0601237 (K.K.); the National Institute of Health under grant R01-CA-142750-01 (K.K.); the Coulter Foundation (K.K.); Taiwan National Health Research Institutes (NHRI) Career Development Grant (CDG) under grant NHRI-EX101-10021EC (Y.-C.T.); Taiwan National Science Council (NSC) under grant 100-2221-E-001-002(Y.-C.T.); the University of Michigan Rackham Predoctoral Fellowship (N.-T.H.); the China PS Foundation under Grant No. 20110490672 and the FP7 European project 247641 (W.J.Z.); the National Natural Science Foundation of China under Grant No. 51071045 and the Program for New Century Excellent Talents in University of Ministry of Education of China under Grant No. NCET-11-0096 (T.Q.); Hong Kong Research Grant Council General Research Funds No. 112510 and City University of Hong Kong Applied Research Grant No. 9667066 (P.K.C.).

References

1 J. Lamb, E. D. Crawford, D. Peck, J. W. Modell, I. C. Blat, M. J. Wrobel, J. Lerner, J. P. Brunet, A. Subramanian, K. N. Ross, M. Reich, H. Hieronymus, G. Wei, S. A. Armstrong, S. J. Haggarty, P. A. Clemons, R. Wei, S. A. Carr, E. S. Lander and T. R. Golub, *Science*, 2006, **313**, 1929–1935.
2 L. A. Loeb, *Nat. Rev. Cancer*, 2011, **11**, 450–457.
3 A. S. Rodrigues, J. Dinis, M. Gromicho, C. Martins, A. Laires and J. Rueff, *Curr. Pharm. Biotechnol.*, 2012, **13**, 651–673.
4 M. Martinez-Rivera and Z. H. Siddik, *Biochem. Pharmacol.*, 2012, **83**, 1049–1062.
5 A. K. Abbas, K. M. Murphy and A. Sher, *Nature*, 1996, **383**, 787–793.
6 K. C. Wood and D. N. Granger, *Clin. Exp. Pharmacol. Physiol.*, 2007, **34**, 926–932.
7 F. Patella and G. Rainaldi, *Cell. Mol. Life Sci.*, 2012, **69**, 1049–1065.
8 H. Clevers, *Nat. Genet.*, 2005, **37**, 1027–1028.
9 P. L. Gourley, *J. Phys. D: Appl. Phys.*, 2003, **36**, R228–R239.
10 X. J. Liang, A. Q. Liu, C. S. Lim, T. C. Ayi and P. H. Yap, *Sens. Actuators, A*, 2007, **133**, 349–354.
11 B. R. Bochner, *Nat. Rev. Genet.*, 2003, **4**, 309–314.
12 E. T. Dermitzakis, *Nature Reviews Genetics*, 2012, **13**, 215–220.
13 D. Psaltis, S. R. Quake and C. Yang, *Nature*, 2006, **442**, 381–386.
14 H. Schmidt and A. R. Hawkins, *Nat. Photonics*, 2011, **5**, 598–604.
15 F. B. Myers and L. P. Lee, *Lab Chip*, 2008, **8**, 2015–2031.
16 X. D. Fan and I. M. White, *Nat. Photonics*, 2011, **5**, 591–597.
17 M.-A. Mycek, B. W. Pogue, *Handbook of Biomedical Fluorescence*, Marcel Dekker, Inc, New York, 2003.
18 B. M. Sauer, J. Hofkens, J. Enderlein, *Handbook of Fluorescence and Imaging: From Ensemble to Single Molecules*, Wiley-VCH, Weinheim, 2011.
19 J. Lippincott-Schwartz and G. H. Patterson, *Science*, 2003, **300**, 87–91.
20 B. Zhu, H. Jia, X. Zhang, Y. Chen, H. Liu and W. Tan, *Anal. Bioanal. Chem.*, 2010, **397**, 1245–1250.
21 R. A. Seder, P. A. Darrah and M. Roederer, *Nat. Rev. Immunol.*, 2008, **8**, 247–258.
22 J. S. Boomer, K. To, K. C. Chang, O. Takasu, D. F. Osborne, A. H. Walton, T. L. Bricker and S. D. Jarman, *JAMA, J. Am. Med. Assoc.*, 2011, **306**, 2594–2605.

23 I. K. Dimov, G. Kijanka, Y. Park, J. Ducree, T. Kang and L. P. Lee, *Lab Chip*, 2011, **11**, 2701–2710.
24 J. Shen, Y. Zhou, T. Lu, J. Peng, Z. Lin, L. Huang, Y. Pang, L. Yu and Y. Huang, *Lab Chip*, 2012, **12**, 317–324.
25 S. Balslev, A. M. Jorgensen, B. Bilenberg, K. B. Mogensen, D. Snakenborg, O. Geschke, J. P. Kutter and A. Kristensen, *Lab Chip*, 2006, **6**, 213–217.
26 Y.-C. Tung, M. Zhang, C.-T. Lin, K. Kurabayashi and S. J. Skerlos, *Sens. Actuators, B*, 2004, **98**, 356–367.
27 J. Seo and L. P. Lee, *Sens. Actuators, B*, 2004, **99**, 615–622.
28 J. A. Chediak, Z. Luo, J. Seo, N. Cheung, L. P. Lee and T. D. Sands, *Sens. Actuators, A*, 2004, **111**, 1–7.
29 O. Schmidt, M. Bassler, P. Kiesel, C. Knollenberg and N. Johnson, *Lab Chip*, 2007, **7**, 626–629.
30 C. V. Raman and K. S. Krishnan, *Nature Genetics*, 1928, **121**, 501–502.
31 J. R. Ferraro, K. Nakamoto, C. R. Brown, *Introductory Raman Spectroscopy*, Second Edition, Elsevier Science, New York, 2003.
32 I. R. Lewis, H. G. M. Edwards, *Handbook of Raman spectroscopy. From the research laboratory to the process line,* Marcel Dekker, New York, 2001.
33 M. Schmitt and J. Popp, *J. Raman Spectrosc.*, 2006, **37**, 20–28.
34 Z. Q. Tian, *J. Raman Spectrosc.*, 2005, **36**, 466–470.
35 A. Otto, I. Mrozek, H. Grabhorn and W. Akemann, *J. Phys.: Condens. Matter*, 1992, **4**, 1143–1212.
36 T. Qiu, W. J. Zhang and P. K. Chu, *Recent Pat. Nanotechnol.*, 2009, **3**, 10–20.
37 M. Moskovits, *Rev. Mod. Phys.*, 1985, **57**, 783–826.
38 K. A. Willets, R. P. Van Duyne, in *Annu. Rev. Phys. Chem.*, Annual Reviews, Palo Alto, 2007, 267–297.
39 X. Qian, X. H. Peng, D. O. Ansari, Q. Yin-Goen, G. Z. Chen, D. M. Shin, L. Yang, A. N. Young, M. D. Wang and S. Nie, *Nat. Biotechnol.*, 2008, **26**, 83–90.
40 D. A. Stuart, J. M. Yuen, N. Shah, O. Lyandres, C. R. Yonzon, M. R. Glucksberg, J. T. Walsh and R. P. V. Duyne, *Anal. Chem.*, 2006, **78**, 7211–7215.
41 L. Chen and J. Choo, *Electrophoresis*, 2008, **29**, 1815–1828.
42 S. Lee, S. Kim, J. Choo, S. Y. Shin, Y. H. Lee, H. Y. Choi, S. Ha, K. Kang and C. H. Oh, *Anal. Chem.*, 2007, **79**, 916–922.
43 K. Lee, V. P. Drachev and J. Irudayaraj, *ACS Nano*, 2011, **5**, 2109–2117.
44 Y. Yin, T. Qiu, W. J. Zhang and P. K. Chu, *J. Mater. Res.*, 2011, **26**, 170–185.
45 G. L. Liu and L. P. Lee, *Appl. Phys. Lett.*, 2005, **87**, 074101.
46 R. A. Frazier, *Handbook of Surface Plasmon Resonance*, RSC Publishing, London, 2008.
47 C. Rivet, H. Lee, A. Hirsch, S. Hamilton and H. Lu, *Chem. Eng. Sci.*, 2011, **66**, 1490–1507.
48 J. Cao, E. K. Galbraith, T. Sun, K. T. V. Grattan, in *Sensors & Their Applications XVI*, 2011.
49 X. Y. Fang, C. L. Liu, X. L. Cheng, Y. L. Wang and Y. C. Yang, *Sens. Actuators, B*, 2011, **156**, 760–764.
50 G. Grasso, R. D'Agata, L. Zanoli and G. Spoto, *Microchem. J.*, 2009, **93**, 82–86.
51 W. Y. Chien, M. Z. Khalid, X. D. Hoa and A. G. Kirk, *Sens. Actuators, B*, 2009, **138**, 441–445.
52 C. J. Huang, K. Bonroy, G. Reekmans, W. Laureyn, K. Verhaegen, I. De Vlaminck, L. Lagae and G. Borghs, *Biomed. Microdevices*, 2009, **11**, 893–901.
53 N. Danz, A. Kick, F. Sonntag, S. Schmieder, B. Hofer, U. Klotzbach and M. Mertig, *Eng. Life Sci.*, 2011, **11**, 566–572.
54 L. Malic, T. Veres and M. Tabrizian, *Biosens. Bioelectron.*, 2011, **26**, 2053–2059.
55 B. E. A. Saleh, M. C. Teich, *Fundamentals of Photonics*, John Wiley & Sons, New York, 1991.
56 R. Barer, *Nature*, 1953, **172**, 1097–1098.
57 V. Backman, M. B. Wallace, L. T. Perelman, J. T. Arendt, R. Gurjar, M. G. Muller, Q. Zhang, G. Zonios, E. Kline, T. McGillican, S. Shapshay, T. Valdez, K. Badizadegan, J. M. Crawford, M. Fitzmaurice, S. Kabani, H. S. Levin, M. Seiler, R. R. Dasari, I. Itzkan, J. Van Dam and M. S. Feld, *Nature*, 2000, **406**, 35–36.
58 R. Bernini, G. Testa, L. Zeni and P. M. Sarro, *Appl. Phys. Lett.*, 2008, **93**, 3.
59 G. Testa, Y. J. Huang, P. M. Sarro, L. Zeni and R. Bernini, *Appl. Phys. Lett.*, 2010, **97**, 3.
60 M. I. Lapsley, I. K. Chiang, Y. B. Zheng, X. Y. Ding, X. L. Mao and T. J. Huang, *Lab Chip*, 2011, **11**, 1795–1800.
61 P. Domachuk, I. C. M. Littler, M. Cronin-Golomb and B. J. Eggleton, *Appl. Phys. Lett.*, 2006, **88**, 3.
62 L. K. Chin, A. Q. Liu, Y. C. Soh, C. S. Lim and C. L. Lin, *Lab Chip*, 2010, **10**, 1072–1078.
63 W. Z. Song and D. Psaltis, *Biomicrofluidics*, 2011, **5**, 11.
64 S. Dante, D. Duval, B. Sepúlveda, A. B. González-Guerrero, J. R. Sendra and L. M. Lechuga, *Opt. Express*, 2012, **20**, 7195–7205.
65 M. Frankowski, N. Bock, A. Kummrow, S. Schadel-Ebner, M. Schmidt, A. Tuchscheerer and J. Neukammer, *Cytometry A*, 2011, **79**, 613–624.
66 N. T. Huang, S. C. Truxal, Y. C. Tung, A. Y. Hsiao, G. D. Luker, S. Takayama and K. Kurabayashi, *Anal. Chem.*, 2010, **82**, 9506–9512.
67 M. Werner, F. Merenda, J. Piguet, R. P. Salathe and H. Vogel, *Lab Chip*, 2011, **11**, 2432–2439.
68 J. Wang, B. Fei, R. L. Geahlen and C. Lu, *Lab Chip*, 2010, **10**, 2673–2679.
69 T. R. Kau, J. C. Way and P. A. Silver, *Nat. Rev. Cancer*, 2004, **4**, 106–117.
70 J. Davis, M. Kakar and C. Lim, *Pharm. Res.*, 2007, **24**, 17–27.
71 M. Rosenauer and M. J. Vellekoop, *Biomicrofluidics*, 2010, **4**, 43005.
72 P. Kiesel, M. Beck and N. Johnson, *Cytometry A*, 2011, **79**, 317–324.
73 P. Kiesel, M. Beck and N. Johnson, *Cytometry, Part A*, 2011, **79A**, 317–324.
74 M. Schelb, C. Vannahme, A. Welle, S. Lenhert, B. Ross and T. Mappes, *J. Biomed. Opt.*, 2010, **15**, 041517.
75 H. Y. Zhu, S. Mavandadi, A. F. Coskun, O. Yaglidere and A. Ozcan, *Anal. Chem.*, 2011, **83**, 6641–6647.
76 C. Ma, R. Fan, H. Ahmad, Q. Shi, B. Comin-Anduix, T. Chodon, R. Koya, C.-C. Liu, G. Kwong, C. Radu, A. Ribas and J. Heath, *Nat. Med.*, 2011, **17**, 738–781.
77 V. Lecault, M. VanInsberghe, S. Sekulovic, D. Knapp, S. Wohrer, W. Bowden, F. Viel, T. McLaughlin, A. Jarandehei, M. Miller, D. Falconnet, A. K. White, D. G. Kent, M. R. Copley, F. Taghipour, C. J. Eaves, R. K. Humphries, J. M. Piret and C. L. Hansen, *Nat. Methods*, 2011, **8**, 581-U593.
78 S. S. Lee, I. A. Vizcarra, D. Huberts, L. P. Lee and M. Heinemann, *Proc. Natl. Acad. Sci. U. S. A.*, 2012, **109**, 4916–4920.
79 P. Skafte-Pedersen, M. Hemmingsen, D. Sabourin, F. S. Blaga, H. Bruus and M. Dufva, *Biomed. Microdevices*, 2012, **14**, 385–399.
80 M. C. Park, J. Y. Hur, H. S. Cho, S. H. Park and K. Y. Suh, *Lab Chip*, 2011, **11**, 79–86.
81 D. Falconnet, A. Niemisto, R. J. Taylor, M. Ricicova, T. Galitski, I. Shmulevich and C. L. Hansen, *Lab Chip*, 2011, **11**, 466–473.
82 X. Zhang, H. Yin, J. M. Cooper and S. J. Haswell, *Anal. Bioanal. Chem.*, 2008, **390**, 833–840.
83 A. Walter, A. März, W. Schumacher, P. Rösch and J. Popp, *Lab Chip*, 2011, **11**, 1013–1021.
84 J. M. Rice, L. J. Stern, E. F. Guignon, D. A. Lawrence and M. A. Lynes, *Biosens. Bioelectron.*, 2012, **31**, 264–269.
85 W. Z. Song, X. M. Zhang, A. Q. Liu, C. S. Lim, P. H. Yap and H. M. M. Hosseini, *Appl. Phys. Lett.*, 2006, **89**, 203901.
86 W. Z. Song, A. Q. Liu, S. Swaminathan, C. S. Lim, P. H. Yap and T. C. Ayi, *Appl. Phys. Lett*, 2007, **91**, 3.
87 H. Shao, W. N. Wang, S. E. Lana and K. L. Lear, *IEEE Photonics Technol. Lett.*, 2008, **20**, 493–495.
88 W. N. Wang, D. W. Kisker, D. H. Thamm, H. Shao and K. L. Lear, *IEEE Trans. Biomed. Eng.*, 2011, **58**, 853–860.
89 W. N. Wang and K. L. Lear, *IEEE J. Sel. Top. Quantum Electron.*, 2010, **16**, 946–953.
90 P. L. Gourley, J. K. Hendricks, A. E. McDonald, R. G. Copeland, K. E. Barrett, C. R. Gourley and R. K. Naviaux, *Biomed. Microdevices*, 2005, **7**, 331–339.
91 P. L. Gourley and R. K. Naviaux, *IEEE J. Sel. Top. Quantum Electron.*, 2005, **11**, 818–826.
92 F. R. Blattner, G. Plunkett, C. A. Bloch, N. T. Perna, V. Burland, M. Riley, J. Collado-Vides, J. D. Glasner, C. K. Rode, G. F. Mayhew, J. Gregor, N. W. Davis, H. A. Kirkpatrick, M. A. Goeden, D. J. Rose, B. Mau and Y. Shao, *Science*, 1997, **277**, 1453–1474.

93 M. D. Adams, *et al.*, , *Science*, 2000, **287**, 2185–2195.
94 S. Kaul, *et al.*, , *Nature*, 2000, **408**, 796–815.
95 E. S. Lander, *et al.*, , *Nature*, 2001, **409**, 860–921.
96 J. C. Venter, *et al.*, , *Science*, 2001, **291**, 1304.
97 R. J. Taylor, D. Falconnet, A. Niemisto, S. A. Ramsey, S. Prinz, I. Shmulevich, T. Galitski and C. L. Hansen, *Proc. Natl. Acad. Sci. U. S. A.*, 2009, **106**, 3758–3763.
98 X. Heng, D. Erickson, L. R. Baugh, Z. Yaqoob, P. W. Sternberg, D. Psaltis and C. H. Yang, *Lab Chip*, 2006, **6**, 1274–1276.
99 X. Q. Cui, L. M. Lee, X. Heng, W. W. Zhong, P. W. Sternberg, D. Psaltis and C. H. Yang, *Proc. Natl. Acad. Sci. U. S. A.*, 2008, **105**, 10670–10675.
100 W. Bishara, S. O. Isikman and A. Ozcan, *Ann. Biomed. Eng.*, 2012, **40**, 251–262.